

# Innovative neutron shielding materials composed of natural rubber-styrene butadiene rubber blends, boron oxide and iron(III) oxide

C Jumpee and D Wongsawaeng<sup>1</sup>

Department of Nuclear Engineering, Faculty of Engineering, Chulalongkorn University, Bangkok, Thailand, 10330

E-mail: doonyapong.w@chula.ac.th

**Abstract.** Optimized flexible and lightweight neutron shielding materials were designed using the Monte Carlo N-Particle (MCNP) code. Thicknesses of 10 mm and 100 mm were tested for neutron shielding performances. Simulation results indicated that the 10 mm shielding material of natural rubber (NR) and styrene butadiene rubber (SBR) blend (1:1) with 60 part per hundred rubber (phr) boron oxide ( $B_2O_3$ ) and 100 mm shielding material with four alternating layers of NR with 100 phr iron (III) oxide ( $Fe_2O_3$ ) and of NR and SBR blend (1:1) with 10 phr  $B_2O_3$  were most suitable for thermal neutron shielding and all-energy neutron shielding, respectively. Experimental results verified the shielding efficiency of these optimal designs and ease of fabrication.

## 1. Introduction

Neutron radiation is widely utilized in medical, agricultural and industrial applications. As neutrons have no electrical charge, they can pass through an electron cloud to interact directly with the atomic nucleus and transfer most of their energy to the nucleus with a mass close to that of a neutron. As the human body has a high water content, there is a high density of hydrogen atoms present. The mass of the hydrogen nucleus is close to that of the neutron. Therefore, exposure to free neutrons can be hazardous, since the interaction of neutrons with molecules in the body can cause disruption to molecules and atoms as well as cause reactions which give rise to other forms of radiation such as protons with high Linear Energy Transfer (LET) [1], [2]. Neutron shielding requires materials with an atomic mass close to that of the neutron. For example, hydrogen-rich materials are often used to shield against neutrons, since ordinary hydrogen both scatters and slows down neutrons, after which neutrons may be absorbed by an isotope exhibiting high affinity for adsorbing slow neutrons such as boron.

There have been several studies of polymeric composition containing materials with high neutron cross section to determine their thermal neutron shielding properties. Materials made of polyethylene or epoxy resin mixed with boron compound are widely used as neutron shielding materials, but they usually exhibit sizable weight and volume, which results in low-flexibility performances [3], [4].

<sup>1</sup> To whom any correspondence should be addressed.



Flexible polymers such as natural rubber (NR) have been used as a matrix for neutron shielding materials, but they only shield against thermal neutrons [5], [6].

There is considerable natural rubber cultivation in many areas of Thailand. This rubber is a hydrocarbon polymer containing a large number of hydrogen atoms and can be easily fabricated into flexible materials. In addition, borate minerals such as boracite, or boron compounds, are found in the northeast of Thailand. Thus, not only is the production of neutron shielding materials comprising natural rubber/ SBR blends and a borate material useful for neutron-related work, but it also utilizes domestic resources.

The most effective neutron shielding material can be obtained by appropriately mixing high hydrogen-content materials, heavy elements and thermal neutron absorbers. High hydrogen-content materials can undergo elastic scattering with fast and intermediate-energy neutrons. Heavy elements can undergo inelastic scattering with fast neutrons and can attenuate the secondary gamma ray emission. Finally, neutron absorbers function to greatly reduce the number of thermal neutrons.

In this experimental work, rubbers, which are low-cost hydrocarbon polymers that can easily be fabricated into many different products and shapes, were selected as the substrate of the composite together with a very low-cost and often disregarded neutron absorbing material,  $B_2O_3$ .  $Fe_2O_3$  (commonly known as rust), a very low-cost and usually disregarded material, was also utilized as the heavy element in the composite.

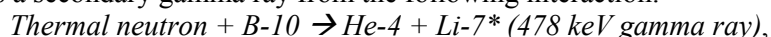
The method of calculation for neutron shielding can be found in references [7], [8]. This research incorporated inelastic scattering and shielding of secondary gamma ray emissions into the simulation. The compositions of neutron shielding materials were optimized by Monte Carlo simulations using the MCNP5 code to examine the neutron flux encompassing the entire range of interaction energy and accounting for secondary gamma ray emissions.

Neutron attenuation experiments were carried out to verify neutron and secondary gamma ray shielding performances of the designed neutron shielding materials using a simulated neutron source (energy  $1 \times 10^{-8} - 100$  MeV) and an Am-Be neutron source.

## 2. Materials and Methods

### 2.1. Material selection and MCNP simulation

The main raw materials were selected from simple elements or compound materials, taking into consideration cost, radiation shielding performances and physical and thermal properties. The main compositions of the selected neutron shielding material to shield against the entire range of neutron energy and secondary gamma ray emission are listed in Table 1. They consisted of natural rubber (NR), styrene butadiene rubber (SBR-1502 from BST elastomer Co., Ltd. Thailand) and neutron absorber/scattering agent [boron oxide ( $B_2O_3$ ), iron(III) oxide ( $Fe_2O_3$ ) and lead dioxide ( $PbO_2$ )]. 40 phr of each agent was used for each sample because preliminary fabrication indicated that at 40 phr, rubber still exhibited desirable properties. The lead or iron content is desirable for inelastic neutron scattering to effectively bring the neutron energy down to lower-energy regions. In addition, lead and iron are used for attenuation of gamma radiation. Neutrons in the lower-energy regions can be moderated by hydrogen and other light elements by elastic scattering. In the thermal energy region, boron (as  $B_2O_3$ ) is used for neutron absorption. Because the interaction between a thermal neutron and boron-10 produces a secondary gamma ray from the following interaction:



without the gamma ray attenuating material (Pb or Fe), this neutron shielding material would itself become a significant source of gamma radiation.

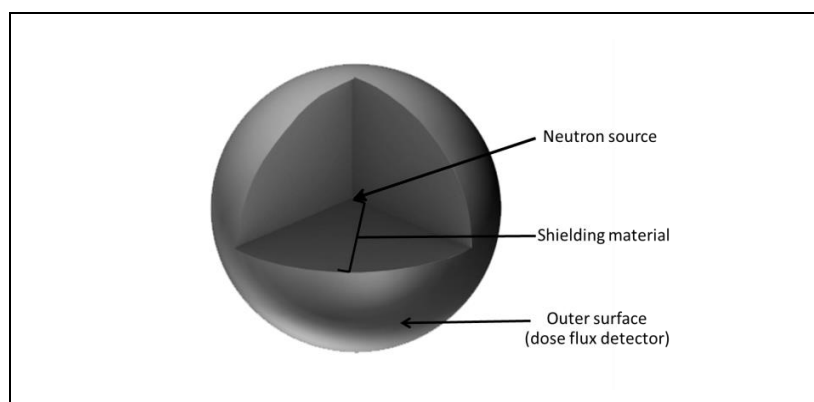
For each sample in table 1, the input card of the MCNP5 transport code was appropriately prepared for testing and comparison of shielding properties of different materials. A simplified model was employed: a single radiation source, an isotropic emission of simulated neutron source with energy  $1 \times 10^{-8} - 100$  MeV, was located at the center of a sphere filled with the shielding material as shown in

figure. 1. The spherical shielding material was considered for shielding the neutron dose equivalent rate [(rem/hr)/source strength] and the secondary gamma dose equivalent rate [(rem/hr)/source strength]. The spherical model of radius 10 mm or 100 mm was chosen for neutron shielding in the thermal region or in the entire-energy range, respectively, to ensure that all neutron particles interacted with the shielding material at least one time before leaving the system. For each shielding material, the dose equivalent rate per source strength was estimated on the outer surface of the sphere.

**Table 1.** Main compositions of considered neutron shielding materials  
(40 phr each of B<sub>2</sub>O<sub>3</sub>, PbO<sub>2</sub> and Fe<sub>2</sub>O<sub>3</sub>)

Sample No.	No. of layers	Material composition	Density (g/cm <sup>3</sup> )	Element content (part per hundred rubber; phr)						
				H	C	B-10	B-11	O	Fe	Pb
0	0	No material (air)	0.00120	Air *						
1	1	NR+SBR	0.987	10.378	89.622	-	-	-	-	-
2	1	NR+SBR+B <sub>2</sub> O <sub>3</sub>	1.210	10.378	89.622	2.460	9.963	27.577	-	-
3	1	NR+SBR+PbO <sub>2</sub>	1.343	10.378	89.622	-	-	5.351	-	34.649
4	1	NR+SBR+Fe <sub>2</sub> O <sub>3</sub>	1.301	10.378	89.622	-	-	12.023	-	13.988
5	1	NR+SBR+B <sub>2</sub> O <sub>3</sub> +PbO <sub>2</sub>	1.273	10.378	89.622	1.230	4.982	16.464	-	17.325
6	1	NR+SBR+B <sub>2</sub> O <sub>3</sub> +Fe <sub>2</sub> O <sub>3</sub>	1.254	10.378	89.622	-	-	19.800	-	27.977
Multi-layer samples										
		Layer 1	Layer 2	Layer 3	Layer 4	Layer 5				
7	4	Sample 2	Sample 3	Sample 2	Sample 3	-				
8	4	Sample 2	Sample 4	Sample 2	Sample 4	-				
9	4	Sample 3	Sample 2	Sample 3	Sample 2	-				
10	4	Sample 4	Sample 2	Sample 4	Sample 2	-				
11	5	Sample 2	Sample 3	Sample 2	Sample 3	Sample 2				
12	5	Sample 2	Sample 4	Sample 4	Sample 4	Sample 2				
13	5	Sample 3	Sample 2	Sample 3	Sample 2	Sample 3				

\*[8] Air's composition (weight fraction) ; Carbon : Nitrogen : Oxygen : Argon  
0.000124 : 0.755268 : 0.231781 : 0.012827



**Figure 1.** Schematic representation of the Monte Carlo model

**Table 2.** Ingredients for fabrication of most appropriate rubber compounds

Ingredient (phr)	Samples						
	1	2	4	10			
				Layer 1	Layer 2	Layer 3	Layer 4
NR	50	50	100	100	50	100	50
SBR-1502	50	50	0	0	50	0	50
ZnO	5	5	5	5	5	5	5
Steric acid	2	2	2	2	2	2	2
Wingstay-L	1	1	1	1	1	1	1
B <sub>2</sub> O <sub>3</sub>	0	60	0	0	10	0	10
Fe <sub>2</sub> O <sub>3</sub>	0	0	5	100	0	100	0
MBTS <sup>a</sup>	1.2	1.2	1.2	1.2	1.2	1.2	1.2
TMTD <sup>b</sup>	1	1	1	1	1	1	1
DPG <sup>c</sup>	0.5	0.5	0.5	0.5	0.5	0.5	0.5
Sulfur	2.5	2.5	2.5	2.5	2.5	2.5	2.5
Compression molded time (min.)	8	30	4	4	15	4	15

<sup>a</sup> Dibenzothiazyl disulphide, <sup>b</sup> Tetramethylthiuram disulphide, <sup>c</sup> Diphenyl Guanidine

## 2.2. Fabrication of the shielding materials

Composite materials shown in table 2, which were the most appropriate rubber compounds after MCNP simulation of all compounds listed in table 1, were fabricated by trial and error, as it was unpredictable which composition would result in a stable compound. All rubber mixtures were prepared in a two-roll mill of 8" x 20" in diameter with the working distance of 300 mm (speed of slow roll 18 rpm) and the gear ratio of 1:4. Powders of B<sub>2</sub>O<sub>3</sub>, PbO<sub>2</sub> and Fe<sub>2</sub>O<sub>3</sub> were appropriately introduced into the blend according to the recipe of compositions given in table 2. Mixing time was about 25 minutes. After compounding, the stock was left for 24 hrs to mature. The sheets were cut into slabs

and then compression molded by an electrically-heated hydraulic press at  $160 \pm 2$  °C and 4 MPa for a suitable duration of each sample.

The homogeneity of each shielding material sample was verified by neutron radiography at the Thai Research Reactor TRR-1/M1, which is a TRIGA-type reactor. A neutron imaging plate (ND 2040) attached to the shielding material by an aluminium tape was exposed to the neutron beam for 4 minutes. The neutron flux and the Cd ratio at the position of the shielding material were approximately  $9 \times 10^5$  n cm<sup>-2</sup> s<sup>-1</sup> and 100, respectively. The neutron imaging plate was processed by an image reader (BAS 2500).

### 2.3. Experimental work on neutron attenuation

The neutron attenuation experiment was carried out at the Radiation Measurement Laboratory at the Nuclear Engineering Department, Faculty of Engineering, Chulalongkorn University to assess neutron shielding performances of the selected shielding materials shown in table 2. Shielding materials were slab shaped with thicknesses of 10 mm and 100 mm and dimensions of 150 mm x 150 mm. These slabs were stacked together to a height of 20 cm. The Am-Be neutron source whose strength was  $3.08 \times 10^3$  n cm<sup>-2</sup> s<sup>-1</sup> was placed at the bottom of the polyethylene (PE) source holder with a distance of 40 mm from the neutron shielding material, as illustrated in figure 2. The neutron measurement was performed using a NE-905 glass scintillation neutron detector connected to a counting system.

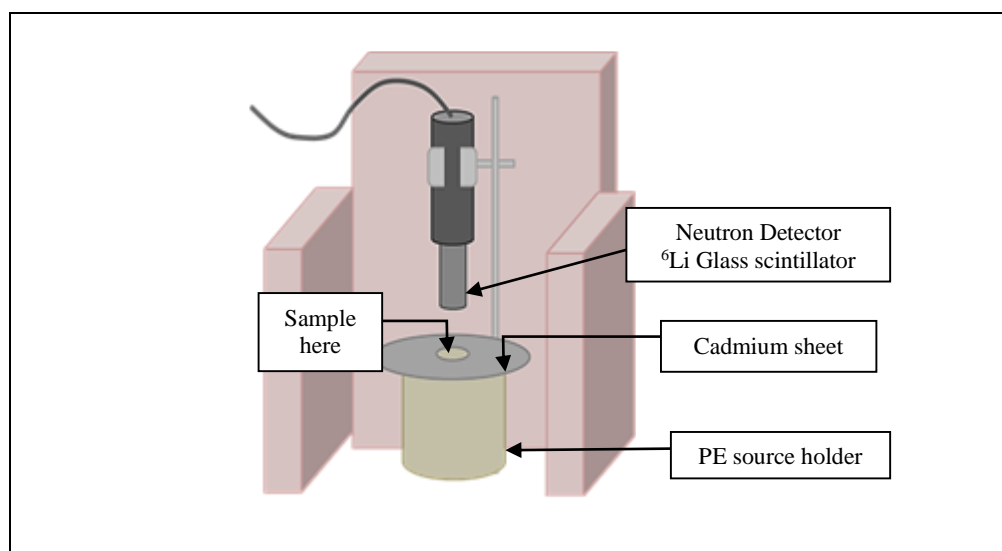


**Figure 2.** Geometry of the neutron transmission test.

## 3. Results and Discussion

### 3.1. MCNP Simulation

Results from the MCNP transport code revealed that the 10-mm thick sample #2 (NR+SBR+B<sub>2</sub>O<sub>3</sub>) and 100-mm thick sample #10 (4 alternating layers of NR+Fe<sub>2</sub>O<sub>3</sub>/NR+SBR+B<sub>2</sub>O<sub>3</sub>) exhibited excellent neutron and secondary gamma ray shielding performances, as seen in figures 3 and 4. For sample #2, because the thickness of 10 mm was smaller than the mean free path of fast neutrons in rubber, only thermal neutrons could be absorbed by this material, which also had the highest boron content. For the 100-mm thick sample #10, fast neutrons could undergo inelastic scattering with iron and elastic scattering with hydrogen present in the rubber to become thermal neutrons and finally be absorbed by boron. Thus, sample #2 and sample #10 are suitable for thermal neutron shielding and all-energy neutron shielding, respectively.

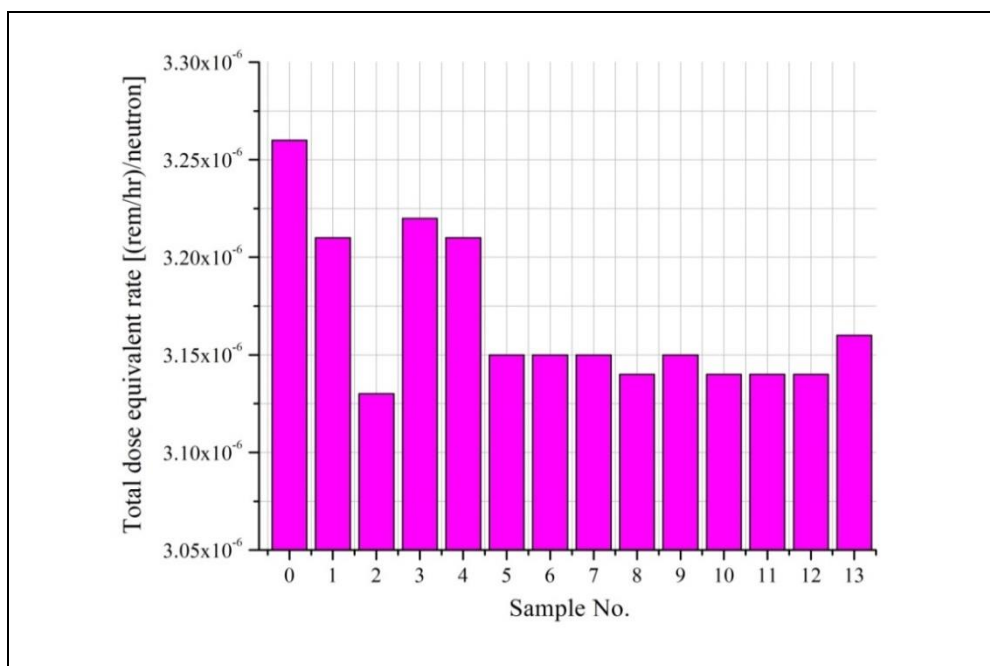


**Figure 3.** Total dose rate equivalent [neutron ( $1 \times 10^{-8}$  – 100 MeV) and secondary photon] on the outer surface of 10-mm radius sphere shielding sample.

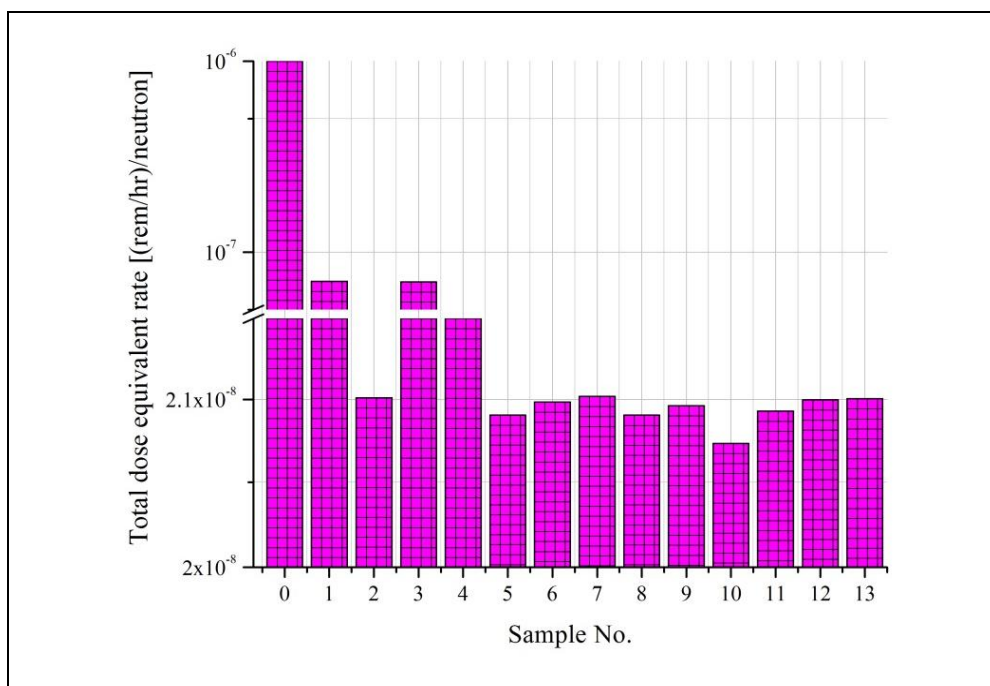
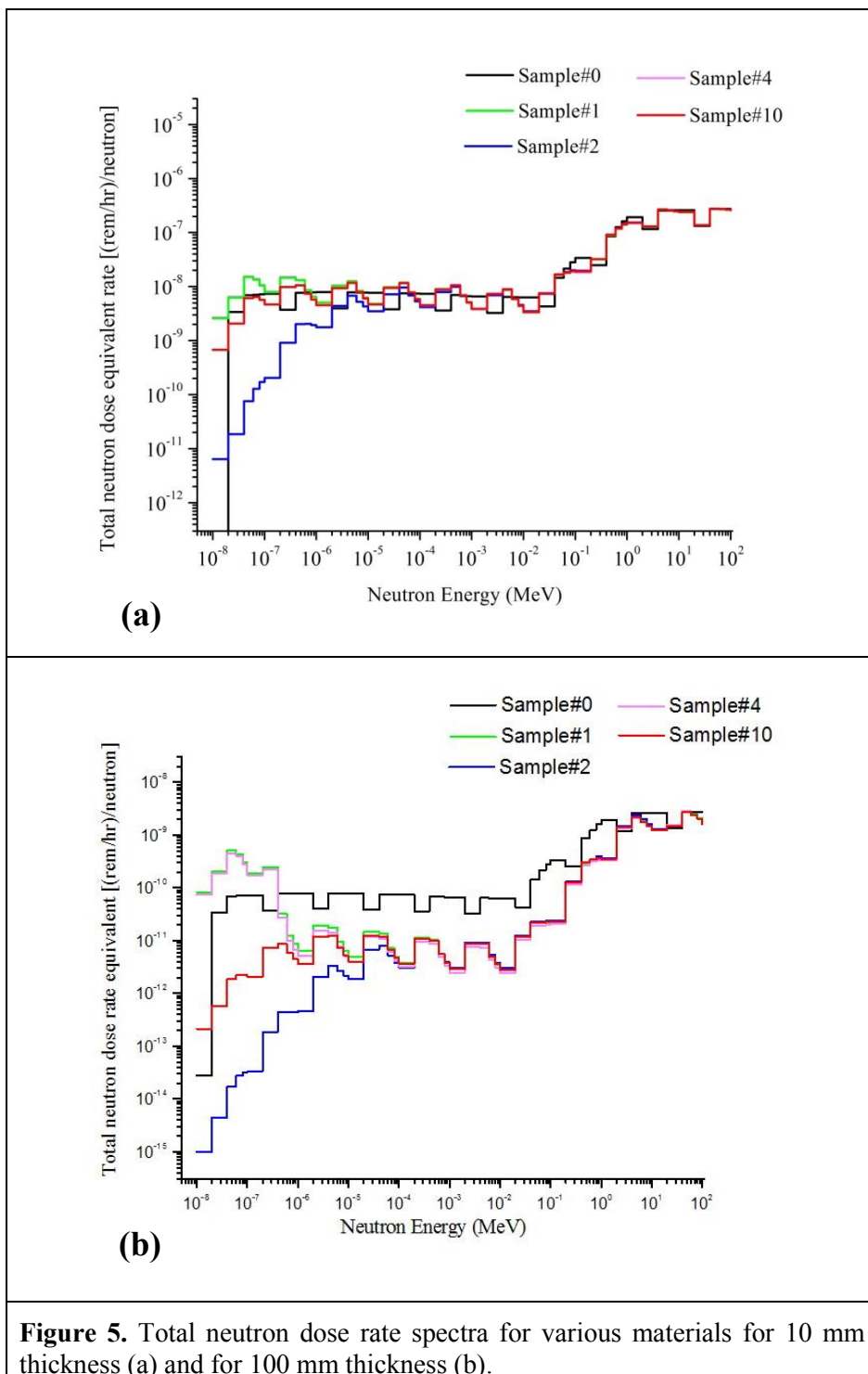


**Figure 4.** Total dose rate equivalent [neutron ( $1 \times 10^{-8}$  100 MeV) and secondary photon] on the outer surface of 100-mm radius sphere shielding sample.



Figures 5(a) and 5(b) illustrate the neutron shielding efficiencies at different energy regions. For sample #2, the best shielding efficiency occurred in the thermal energy range ( $1 \times 10^{-8} - 1 \times 10^{-2}$  MeV) because boron exhibits a high thermal neutron absorption cross-section. In the fast neutron regime ( $1 \times 10^{-1} - 1 \times 10^2$  MeV), for 100-mm thick shielding designs, although not clearly visible in Figure 5(b),

sample #10 outperformed sample #2 because the total neutron dose rate equivalent was lower in the entire fast neutron energy range. Moreover, for sample #10, it also performed better than the NR/SBR rubber compound (sample #1) and NR/SBR/Fe<sub>2</sub>O<sub>3</sub> (sample #4) in the thermal energy range due to the presence of the boron compound.

To further determine the optimized amount of B<sub>2</sub>O<sub>3</sub> and Fe<sub>2</sub>O<sub>3</sub> additions, a simulation of a 10 mm thick sample #2 with varying amounts of B<sub>2</sub>O<sub>3</sub> added from 0 to 70 phr was performed. Results are shown in figure 6(a). As more B<sub>2</sub>O<sub>3</sub> was added, the total dose rate equivalent became reduced and appeared to saturate after about 60 phr. Thus, the most appropriate B<sub>2</sub>O<sub>3</sub> addition for sample #2 was chosen to be 60 phr. Moreover, a simulation of a 100 mm thick sample #10 with varying amounts of B<sub>2</sub>O<sub>3</sub> added from 0 to 70 phr and Fe<sub>2</sub>O<sub>3</sub> added from 0 to 100 phr was performed. The reason why the amount of Fe<sub>2</sub>O<sub>3</sub> added was limited to 100 phr was because during a trial fabrication test, the rubber became very rigid at 100 phr and more, making it much less flexible. Results in figure 6(b) revealed that the most appropriate amounts were 100 phr of Fe<sub>2</sub>O<sub>3</sub> and 10 phr of B<sub>2</sub>O<sub>3</sub>.

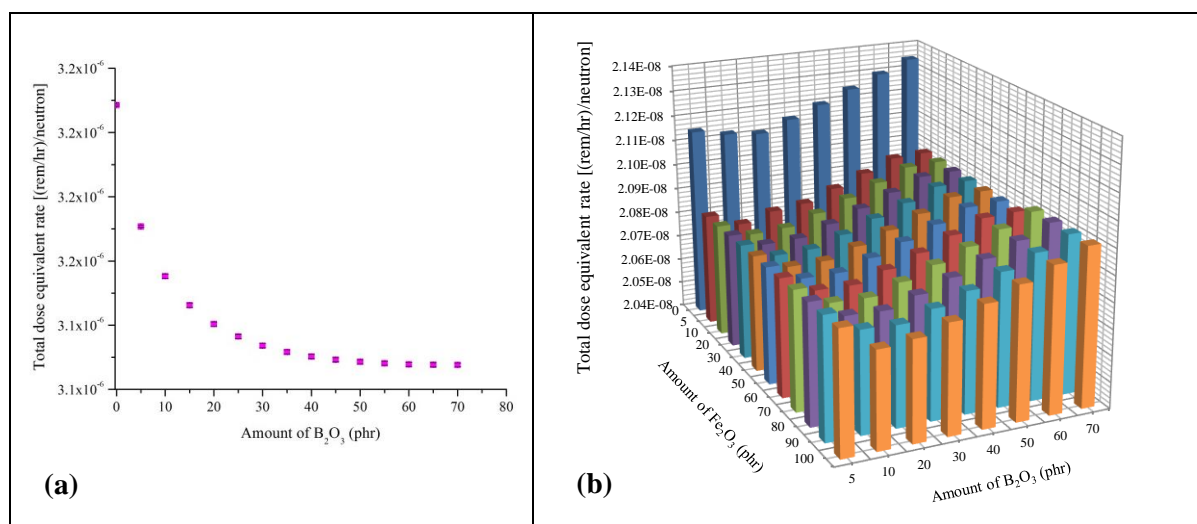


**Figure 6.** Total dose rate on outer surface of sphere neutron shielding at different mass ratios of neutron absorber contents (Part per hundred rubber; phr) for (a) 10 mm of sample#2 and (b) 100 mm of sample#10.

### 3.2. Fabrication of rubber compound

The optimized designs according to the MCNP simulation were fabricated by trial and error. The successfully-fabricated shielding materials with slab geometry are shown in figures 7(a) and 8(a). Homogeneity was one of several factors determining the suitability of the fabricated shielding materials. In reality, for the rubber compounds of samples #2 and #10, if they were left exposed to moisture in room condition, B<sub>2</sub>O<sub>3</sub> would quickly react with water vapour in the atmosphere, turning into boric acid crystals, causing a problem with homogeneity. Thus, the samples must be completely encased in a thin layer of conventional rubber compound. Therefore, figure 7(a) represents the rubber compound encased in the green conventional rubber. In figure 8(a), because the rubber with iron oxide didn't require any encasement, the red slab represented the actual rubber compound. The corresponding neutron radiographs displayed in figures 7(b) and 8(b) exhibiting a very even color tone indicated that the neutron absorbing/scattering materials (B<sub>2</sub>O<sub>3</sub> or Fe<sub>2</sub>O<sub>3</sub>) can be homogeneously dispersed in the rubber compounds of NR and SBR.





**Figure 7.** (a) Front view and (b) side view of 10 mm (NR+SBR+B<sub>2</sub>O<sub>3</sub> 60 PHR: sample#2) shielding material samples trial-produced to fabricate slab shape. (c) Neutron radiograph of this shielding material (front view).

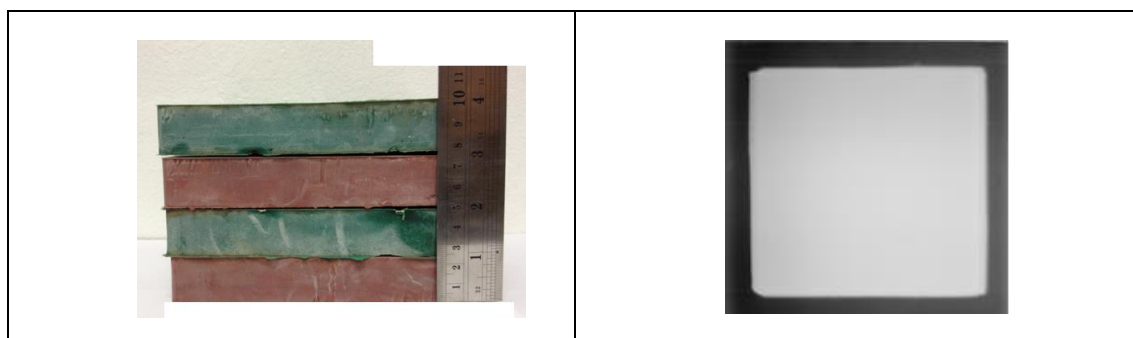


**Figure 8.** (a) Side view of 100 mm (4 layers: sample#10) shielding material samples trial-produced to fabricate slab shape. (b) Neutron radiograph of this shielding material.

### 3.3. Neutron transmission test

From the neutron transmission test, the 10 mm rubber compound with 60 phr of B<sub>2</sub>O<sub>3</sub> can reduce the neutron dose from the Am-Be source by 53.91%. The 100 mm rubber compound composed of 4 alternating layers with 100 phr Fe<sub>2</sub>O<sub>3</sub> and 20 phr B<sub>2</sub>O<sub>3</sub> can reduce the neutron dose by 72.56%.

## 4. Conclusion

Optimized flexible and lightweight neutron shielding materials were designed using the MCNP code. The neutron shielding materials with thicknesses of 10 mm and 100 mm were examined for neutron shielding performances. Simulation results indicate that the 10 mm shielding material of NR and SBR blend (1:1) with 60 phr B<sub>2</sub>O<sub>3</sub>, and the 100 mm shielding material having 4 alternating layers of NR with 100 phr Fe<sub>2</sub>O<sub>3</sub> and of NR and SBR blend (1:1) with 10 phr B<sub>2</sub>O<sub>3</sub> were most suitable for thermal neutron shielding and all-energy neutron shielding, respectively. Experimental results verified the shielding efficiency of these optimal designs and the ease of fabrication. The designed shielding materials are highly suitable for applications in nuclear science and technology.

## Acknowledgments

This work was financially supported by the Graduate School, Chulalongkorn University and The Commission on Higher Education under Strategic Scholarships for Frontier Research Network for the Thai Ph.D. Doctoral Degree Program.

## References

- [1] Kenneth S J and Faw R 2000 *Radiation Shielding* (Illinois: American Nuclear Society)
- [2] Knoll G 1979 *Radiation Detection and Measurement* (Toronto: John Wiley & Sons)
- [3] Koichi O 2005 Neutron shielding material based on colemanite and epoxy resin *Radiat Prot Dosimetry* **115** 258–61
- [4] Gwaily S E, Badawy M M, Hassan H H and Madani M 2002 Natural rubber composites as thermal neutron radiation shields II —  $\text{H}_3\text{BO}_3/\text{NR}$  composites *Polym Test* **21** 513-17
- [5] Gwaily S E, Badawy M M, Hassan H H and Madani M 2002 Natural rubber composites as thermal neutron radiation Shields I.  $\text{B}_4\text{C}/\text{NR}$  composites *Polym Test* **21** 129-33
- [6] Huasi H *et al* 2008 Study on composite material for shielding mixed neutron and gamma rays *IEEE Trans Nucl Sci* **55** 4
- [7] Elbio C, Florian G, Burkhard S, Harald T 2011 Reusable shielding material for neutron- and gamma-radiation *Nucl Instrum Methods Phys Res A* **651** 77-80
- [8] McConn Jr R J, Gesh C J, Pagh R T, Rucker R A and Wlliams III R G 2011 *Radiation portal monitor project: Compendium of material composition data for radiation transport modelling* (Washington: Pacific Northwest National Laboratory)